

# Hydrogen and the Structure of the Transition Aluminas

Karl Sohlberg,<sup>\*,†</sup> Stephen J. Pennycook,<sup>†,‡</sup> and Sokrates T. Pantelides<sup>†,‡</sup>

Contribution from the Solid State Division, P.O. Box 2008, Oak Ridge National Laboratory, Oak Ridge, Tennessee 37831-6031, and Department of Physics and Astronomy, Vanderbilt University, Nashville, Tennessee 37235

Received April 7, 1999. Revised Manuscript Received June 17, 1999

**Abstract:**  $\alpha$ -Alumina results from the complete dehydration of several minerals of the form  $\text{Al}_2\text{O}_3 \cdot n\text{H}_2\text{O}$ . The “transition” aluminas,  $\gamma$ -alumina,  $\eta$ -alumina, and  $\delta$ -alumina are known to have a spinel structure but the possibility that they contain hydrogen (H) has been the subject of debate. We present a series of density-functional theory calculations which, together with available experimental data, show that the spinel aluminas exist over a range of hydrogen content captured by the empirical formula  $\text{H}_{3m}\text{Al}_{2-m}\text{O}_3$ , with different greek-letter phases corresponding to different distributions of the Aluminum (Al) ions on the two cation sublattices. Calculations of densities and vibrational frequencies of bulk OH bonds are in excellent agreement with available data. The theory reconciles seemingly inconsistent data and reveals a remarkable property of the spinel aluminas: They are “reactive sponges” in that they can store and release water in a reactive way. This chemical activity offers a basis for understanding long-standing puzzles in the behavior of aluminas in catalytic systems.

## 1. Introduction

$\gamma$ -Alumina is without question an enormously important material in catalysis. For example, it is used as a catalyst in hydrocarbon conversion<sup>1,2</sup> (petroleum refining), and as a support for automotive<sup>3,4</sup> and industrial catalysts.<sup>5,6</sup> In particular, catalytic reduction of automotive pollutants such as nitric oxide ( $\text{NO}_x$ ), as well as oxidation of carbon monoxide (CO) and hydrocarbons (HC), is accomplished with transition-metal elements such as platinum (Pt), rhodium (Rh), or palladium (Pd) dispersed on  $\gamma$ -alumina surfaces.<sup>7–10</sup> Industrial process catalysts for such processes as olefin isomerization,<sup>11,12</sup> alcohol dehydration,<sup>13,14</sup> and oxidation of organics<sup>15</sup> are also formed by dispersal of transition-metal atoms on a  $\gamma$ -alumina surface. Remarkably, despite its widespread use, its structure and composition remain unresolved.<sup>16–18</sup> In general, there are two schools of thought

concerning the composition of  $\gamma$ -alumina, although controversy over the structure exists within each camp. The most widely held view is that  $\gamma$ -alumina is a stoichiometric oxide of aluminum with a defect spinel structure. A minority view is that  $\gamma$ -alumina actually contains hydrogen. In this paper, we present a comprehensive and systematic description of  $\gamma$ -alumina based on density functional theory (DFT) calculations in terms of which we can reconcile the two seemingly contradictory interpretations of experimental data. Our systematic description also clarifies the relationship of  $\gamma$ -alumina to some of the other transition aluminas, and provides clues to its success as a catalyst and catalytic support. To place the present work into context, it is useful to first detail the controversy that exists over the composition and structure of  $\gamma$ -alumina.

The first point of view, obtained originally through X-ray diffraction, is that  $\gamma$ -alumina has a defect spinel structure. It was established as early as 1935 that the structure of  $\gamma$ -alumina is closely related to that of magnesium spinel ( $\text{MgAl}_2\text{O}_4$ ). Spinel has 24 cations and 32 anions in a cubic unit cell. The oxygen (O) atoms are close-packed, with the magnesium (Mg) atoms occupying tetrahedral ( $T_d$ ) sites and the Aluminum (Al) atoms occupying octahedral ( $O_h$ ) sites.<sup>19</sup> In  $\gamma$ -alumina, Al atoms occupy both the tetrahedral and octahedral cation positions among the cubic close-packed oxygens. To satisfy the  $\text{Al}_2\text{O}_3$  stoichiometry of aluminum oxide, however, in  $\gamma$ -alumina  $2^{2/3}$  of the 24 cation sites need to be vacant. The formula for  $\gamma$ -alumina is, therefore, typically given as  $\square_{2^{2/3}}\text{Al}_{21^{1/3}}\text{O}_{32}$ , where  $\square$  stands for a vacancy. Within this camp controversy remains over the distribution of the vacancies over the two cation sublattices.

The second point of view comes from chemical analysis. While the majority view is that  $\gamma$ -alumina is a stoichiometric oxide of aluminum, there have been intermittent reports that  $\gamma$ -alumina actually contains hydrogen (H) in its composition. These reports, therefore, cast doubt on the validity of the widely accepted defect spinel structure.

(19) Wyckoff, R. W. G. *Crystal Structures*; Interscience: New York, 1963.

<sup>†</sup> Oakridge National Laboratory.

<sup>‡</sup> Vanderbilt University.

- (1) Knözinger, H.; Ratnasamy, P. *Catal. Rev.—Sci. Eng.* **1978**, *17*, 31.
- (2) Tung, S. E.; Mcininch, E. J. *Catal.* **1964**, *3*, 229.
- (3) Satterfield, C. N. *Heterogeneous Catalysis in Practice*; McGraw-Hill: New York, 1980; Section 4.5.
- (4) Gates, B. C. *Chem. Rev.* **1995**, *95*, 511.
- (5) Che, M.; Bennett, C. O. *Adv. Catal.* **1989**, *36*, 55.
- (6) Xu, Z.; Xiao, F.-S.; Purnell, S. K.; Alexeev, O.; Kawi, S.; Deutsch, S. E.; Gates, B. C. *Nature* **1994**, *372*, 346.
- (7) Kummer, J. T. *Prog. Energy Combust. Sci.* **1980**, *6*, 177.
- (8) Cooper, B. J. *Platinum Met. Rev.* **1994**, *38*, 2.
- (9) McCabe, R. W.; Usmen, R. K.; Ober, K.; Gandhi, H. S. *J. Catal.* **1995**, *151*, 385.
- (10) Taylor, K. C. *Catal. Rev.—Sci. Eng.* **1993**, *35*, 457.
- (11) Ivey, M. M.; Allen, H. C.; Avoyan, A.; Martin, K. A.; Hemminger, J. C. *J. Am. Chem. Soc.* **1998**, *120*, 10980.
- (12) Trombetta, M.; Busca, G.; Rossini, S.; Piccoli, V.; Cornaro, U.; Guercio, A.; Catani, R.; Willey, R. J. *J. Catal.* **1998**, *179*, 581.
- (13) Knözinger, H. *Angew. Chem., Int. Ed. Engl.* **1968**, *7*, 791.
- (14) Shi, B.; Davis, B. H. *J. Catal.* **1995**, *157*, 359.
- (15) Busca, G. *Catal. Today* **1996**, *27*, 457.
- (16) Wefers, K.; Misra, C. *Oxides and Hydroxides of Aluminum*; Alcoa Laboratories: Pittsburgh, PA, 1987.
- (17) Henrich, V. E.; Cox, P. A. *The Surface Science of Metal Oxides*; Cambridge University Press: Cambridge, 1994; Section 2.3.
- (18) Tsyganenko, A. A.; Mardilovich, P. P. *J. Chem. Soc., Faraday Trans.* **1996**, *92*, 4843.

The first mention of H was made by Dowden in 1950,<sup>20</sup> who suggested that protons might reside in the cation vacancies. Several authors have since proposed that the formula for  $\gamma$ -alumina can be written  $\text{Al}_2\text{O}_3 \cdot n\text{H}_2\text{O}$ .<sup>21–24</sup> This notation conveys that upon dehydration  $\gamma$ -alumina produces stoichiometric alumina. Unfortunately, it also suggests that  $\gamma$ -alumina is a crystalline hydrate, although it is widely recognized that this is not the case.<sup>22</sup> (Below we will present a new formula that more accurately conveys the chemistry of dehydration.)

To determine the distribution of protons between the surface and the bulk, Pearson<sup>25</sup> performed proton NMR measurements on two trademarked transition aluminas. The concentration of H was reported to be (0.00888 g H)/(g alumina), with 63.2% of the H on the surface. This distribution translates to  $n = 0.18$ .

Using X-ray diffraction, DeBoer and Houben<sup>21</sup> observed that for values of ( $0.051 \leq n \leq 0.63$ ) the spinel lattice is preserved. They also measured the material density as a function of  $n$  and noted that  $\text{Al}_2\text{O}_3 \cdot \frac{1}{5}\text{H}_2\text{O}$  is a special form. In this case ( $n = 0.2$ ) the formula can be written  $\text{HAl}_5\text{O}_8$ , a perfect H spinel with no vacancies.

An important contribution was made by Soled<sup>22</sup> who measured weight loss of  $\gamma$ -alumina upon thermal conversion to  $\alpha$ -alumina (corundum). He attributed the weight loss to water expulsion and concluded that  $n = \frac{1}{5}$  in the above formula. On the basis of a similar dehydration experiment, Zhou and Snyder<sup>24</sup> report the formula  $\text{Al}_2\text{O}_3 \cdot 0.048(\text{H}_2\text{O})$  for  $\gamma$ -alumina.

Ushakov and Moroz attempted to settle the issue of octahedral vs tetrahedral vacancies by the profile refinement method (PRF), whereby the X-ray diffraction pattern predicted from a structural model is compared to an experimental one.<sup>23</sup> They found that no distribution of vacancies between octahedral and tetrahedral sites produced a predicted X-ray diffraction pattern in agreement with experiments. Only when H was included in the bulk model (which reduces the Al concentration), was good agreement achieved. They concluded that the formula for  $\gamma$ -alumina can be written formally as  $\text{Al}_2\text{O}_3 \cdot n\text{H}_2\text{O}$ , where  $0 \leq n \leq 0.6$ .

Some of the most convincing evidence for H within the bulk of  $\gamma$ -alumina comes from the work of Tsyganenko *et al.*<sup>26</sup> They detected characteristic OH vibrational absorption bands in the IR spectrum of  $\gamma$ -alumina and monitored their evolution with increasing temperature. Through isotopic substitution of H with D, they were able to distinguish surface OH from OH within the bulk. They attributed two observed bands to OH ions with the H at a nominal tetrahedral or octahedral cation site in the spinel lattice.

All experimental evidence points to the fact that, independent of the value of  $n$ , the spinel O sublattice is complete, but a fraction of Al atoms are missing. A description that unifies all of these earlier findings is that there is a range of valid H-content, and H is compensated for by an Al deficiency so that an appropriate formula for the sequence is  $\text{H}_{3m}\text{Al}_{2-m}\text{O}_3$ , where  $m = 2n/(n + 3)$ . We contrast this formula with  $\text{Al}_2\text{O}_3 \cdot n\text{H}_2\text{O}$ . The  $\text{Al}_2\text{O}_3 \cdot n\text{H}_2\text{O}$  notation conveys the incorrect notion that excess O is involved in conjunction with the presence of H. The formula  $\text{H}_{3m}\text{Al}_{2-m}\text{O}_3$  not only provides an appropriate description of the composition but also provides, for the first

time, a mechanism for dehydration. For every three H atoms that go out, one Al atom must go in from the surface to satisfy valence requirements. This mechanism leads to very unusual surface chemistry as will be described later.

## 2. Theoretical Method

The present electronic structure calculations were based on density functional theory<sup>27</sup> with the generalized gradient approximation (GGA) to the exchange-correlation energy,<sup>28</sup> as recently reviewed by Payne *et al.*,<sup>29</sup> and implemented in the program CASTEP.<sup>29</sup> The electron-ion interactions were described with nonlocal reciprocal-space pseudopotentials in the Kleinman–Bylander form.<sup>30</sup> The electronic density was expanded in a plane wave basis truncated subject to a 1500 eV cutoff energy. Convergence tests were performed, and this cutoff energy was determined to be sufficiently high to obtain consistency between the stress and energy minima upon ionic relaxation. Integrations over the Brillouin zone employed a grid of  $k$ -points with a spacing of  $0.1 \text{ \AA}^{-1}$  chosen according to the Monkhorst–Pack scheme.<sup>31</sup>

Vibrational frequencies for H were computed in the harmonic approximation by diagonalizing the mass-weighted Cartesian force constant matrix applicable to the H atom in question.<sup>32</sup> The Cartesian force constants were approximated by computing divided-difference numerical second derivatives of the potential. The step size for the numerical differentiation was taken as  $0.01 \text{ \AA}$ .

## 3. Results

Three sets of calculations were undertaken. First, fully relaxed structures (including unit cell optimization) were computed for  $\gamma$ -alumina at various levels of dehydration. Second, vibrational frequencies were computed for hydrogen atoms within the bulk. Third, the energy barrier to diffusion of hydrogen through the bulk was computed. In all cases, the results of these calculations can be related to physical observables.

**3.1. Total Energy versus “Water” Content.** As discussed above, several previous reports have suggested that the composition of  $\gamma$ -alumina may be expressed formally as  $\text{Al}_2\text{O}_3 \cdot n\text{H}_2\text{O}$ . There is, however, no consensus concerning the correct value for  $n$ , and in at least one case it was implied that a range of values may be valid.<sup>21</sup> We have found that there is indeed a sequence of forms, and the key to understanding this sequence is to understand the structure for  $n = 0.2$ . In this case, the empirical formula is  $\text{HAl}_5\text{O}_8$ . As noted above, this is a perfect spinel structure with all cation sites occupied. It is most easily described in terms of the closely related Mg spinel. The cubic cell of Mg spinel has 24 cations and 32 anions, ( $\text{Mg}_8\text{Al}_{16}\text{O}_{32}$ ) but the *primitive* unit cell is a rhombohedron with the contents  $\text{Mg}_2\text{Al}_4\text{O}_8$ . (See Figure 1.) The space group is  $Fd\bar{3}m$ .<sup>19</sup> Two possible primitive cells for  $\text{HAl}_5\text{O}_8$  can be described in terms of the Mg spinel primitive cell as follows:  $\text{HAl}_5\text{O}_8 (T_d)$  is generated by starting with Mg spinel and replacing half of the Mg with Al and the other half with H. Note that in this case the H atom has nominal  $T_d$  coordination.  $\text{HAl}_5\text{O}_8 (O_h)$  is generated by starting with Mg spinel, replacing one of the Al atoms with an H atom and then replacing all of the Mg by Al. Here the nominal coordination of the H atom is  $O_h$ . In both cases, *all* of the spinel cation sites are occupied. The  $\text{HAl}_5\text{O}_8$  forms are therefore not defect structures.

We have computed fully relaxed structures for both the  $\text{HAl}_5\text{O}_8 (T_d)$  and  $\text{HAl}_5\text{O}_8 (O_h)$  forms, starting from the Mg spinel

(20) Dowden, D. A. *J. Chem. Soc.* **1950**, 1–2, 242.

(21) de Boer, J. H.; Houben, G. M. M. *Proc. Int. Symp. React. Solids* **1952**, 1, 237.

(22) Soled, S. *J. Catal.* **1983**, 81, 252.

(23) Ushakov, V. A.; Moroz, E. M. *React. Kinet. Catal. Lett.* **1984**, 24, 113.

(24) Zhou, R–S.; Snyder, R. L. *Acta Crystallogr.* **1991**, B47, 617.

(25) Pearson, R. M. *J. Catal.* **1971**, 23, 388.

(26) Tsyganenko, A. A.; Smirnov, K. S.; Rzhvskij, A. M.; Mardilovich, P. P. *Mater. Chem. Phys.* **1990**, 26, 35.

(27) Kohn, W.; Sham, L. J. *Phys. Rev.* **1965**, 140A, 1133.

(28) Perdew, J. P. *Phys. Rev. B* **1986**, 33, 8822.

(29) Payne, M. C.; Teter, M. P.; Allan, D. C.; Arias, T. A.; Joannopoulos, J. D. *Rev. Mod. Phys.* **1992**, 64, 1045.

(30) Kleinman, L.; Bylander, D. M. *Phys. Rev. Lett.* **1982**, 48, 1425.

(31) Monkhorst, H. J.; Pack, J. D. *Phys. Rev. B* **1976**, 13, 5188.

(32) Califano, S. *Vibrational States*; Wiley: London, 1976.

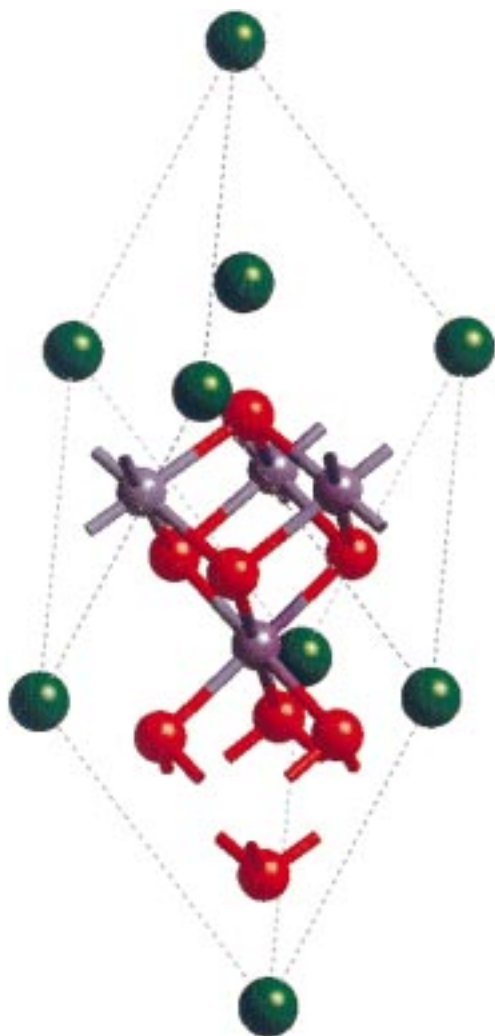


**Figure 1.** Primitive unit cell for Mg spinel ( $\text{Mg}_2\text{Al}_4\text{O}_8$ ). The Mg atoms (green) are tetrahedrally coordinated by O (red), and the Al (blue) atoms are octahedrally coordinated by O.

structure and constructing the hydrogen-containing forms as described above. We have found that both forms are stable, although the H atoms relax substantially from the ideal spinel cation sites. In both cases the H atom associates more closely with *one* of the nearest neighbor O atoms, forming a OH-type structure within the bulk, the closest O–H distance being about 0.97 Å in both cases, (within the precision of the present calculations). These are therefore essentially true OH groups, they are not bridged structures.

Values of  $n < 0.2$  and  $n > 0.2$  represent defect forms. In particular, smaller values of  $n$  correspond to three H atoms at a time being replaced by an Al atom and two vacancies. Clearly the primitive cell must have a different size each time such an exchange is completed. For example, start with four units of  $\text{HAl}_5\text{O}_8$  and replace three H with an Al and two vacancies. The new stoichiometry is  $\text{H}_1\text{Al}_2\text{Al}_2\text{O}_{32}$  and corresponds to 10.5 units of  $\text{Al}_2\text{O}_3 \cdot \frac{1}{21}\text{H}_2\text{O} = \text{Al}_2\text{O}_3 \cdot 0.048\text{H}_2\text{O}$ . Values of  $n > 0.2$  correspond to an Al atom being replaced by three H atoms. Again, the primitive cell must have a different size each time such an exchange is completed. For example, start with four units of  $\text{HAl}_5\text{O}_8$ , remove one Al and insert three H. The new stoichiometry is  $\text{H}_7\text{Al}_9\text{O}_{32}$ , and corresponds to  $\text{Al}_2\text{O}_3 \cdot \frac{7}{19}\text{H}_2\text{O}$ , ( $n \approx 0.368$ ). The value  $n = 0.2$  marks the division between forms which are poor in H with respect to the perfect H spinel and therefore contain vacancies and structures which are rich

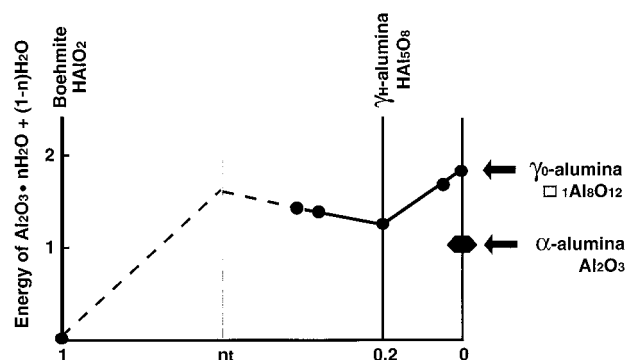


**Figure 2.** Energy diagram for the transition of boehmite to  $\gamma$ -alumina and ultimately, corundum. The total energies of the various structures, given relative to boehmite = 0.00, are:  $\alpha$ -alumina = 1.00 eV,  $\gamma_0$ -alumina = 1.81 eV,  $\gamma_{0.048}$ -alumina = 1.69 eV,  $\gamma_{0.2}$ -alumina = 1.29 eV,  $\gamma_{0.368}$ -alumina = 1.39 eV,  $\gamma_{0.429}$ -alumina = 1.40 eV. Here the energies are reported for:  $\text{Al}_2\text{O}_3 \cdot n(\text{H}_2\text{O}) + (1-n)\text{H}_2\text{O}$ . All structures are fully relaxed. At some point during the dehydration of boehmite, shown schematically by the broken line, a transformation occurs to the spinel structure. The transformation is denoted  $n$ , here and most likely takes place at  $n_t \approx 0.6$ .

in hydrogen with respect to the perfect spinel and therefore contain interstitial H atoms.

In the H-poor regime, there is a net concentration of vacant cation sites. For  $n > 0.2$  ( $m > 0.125$ ), the H-rich regime, all cation sites are nominally occupied, plus there is an excess concentration of H atoms. To denote these facts explicitly in the formulas, we introduce a new index  $k = 5n/2$ , in terms which the H-poor compounds ( $k < 0.5$ ) are written as  $\square_{1-2k}\text{H}_{3k}\text{Al}_{8-k}\text{O}_{12}$  and the H-rich compounds ( $k > 0.5$ ) are written as  $\hat{\text{H}}_{2k-1}\text{H}_{3k}\text{Al}_{8-k}\text{O}_{12}$ , where  $\hat{\text{H}}$  denotes the excess H atoms.

We have computed total energies for a range of values of  $n$ , constructing the primitive unit cells as described in the preceding paragraphs. The results are depicted in Figure 2. For a relative comparison of energies it is necessary to have the same number of atoms in each calculation. It is therefore convenient to plot the energy of  $\text{Al}_2\text{O}_3 \cdot n\text{H}_2\text{O} + (1-n)\text{H}_2\text{O}$  as function of  $n$ . An added advantage of plotting the total energies as a function of  $n$  is that both the precursor material, boehmite, and the ultimate dehydration product, corundum ( $\alpha$ -alumina), can be conveniently included on the same plot. The lowest-energy structure is boehmite, which is consistent with the fact that boehmite is a natural mineral.<sup>33</sup> We define this energy as the zero of our energy scale. In completely dehydrated form, the lowest-energy structure is  $\alpha$ -alumina (hexagonal structure), again in agreement with observations. It is 1.0 eV above boehmite. Note that there is a local minimum in the curve at  $n = 0.2$ , the perfect H spinel structure. Deviations from  $n = 0.2$ , whether positive or negative, introduce defects into the structure and therefore increase the total energy. The fact that the total energy curve is computed to be essentially linear in the region  $[0.0 \leq n \leq 0.2]$  suggests that the H atoms are noninteracting, consistent with the fact that there is just one H atom per primitive unit cell.

The fully optimized total energy calculations also yield the material density. (One needs to know only the volume of the unit cell and its contents to compute density.) The computed variation in density with  $n$  is given in Figure 3, where it is compared with the experimental results of de Boer and Houben.<sup>21</sup> There is a systematic error in the calculation due to an error of about 6% in the lattice constant, but the trend is reproduced with high accuracy. This systematic error is a well-

(33) Hill, R. J. *Clays Clay Min.* **1981**, 29, 435.



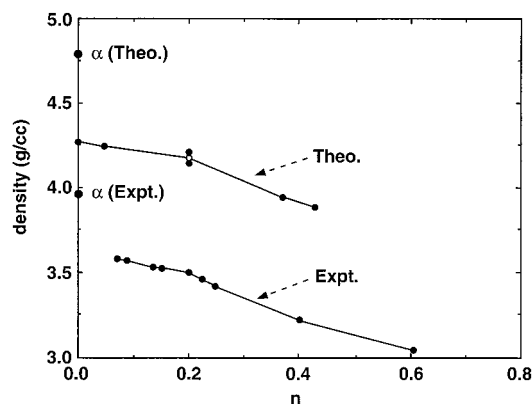


**Figure 3.** Computed and experimental<sup>21</sup> densities for  $\text{Al}_2\text{O}_3 \cdot n(\text{H}_2\text{O})$  as a function of  $n$ . Computed and experimental densities for  $\alpha$ -alumina are also shown for comparison. The multiple points at  $n = 0.2$  are for different distributions of Al over the tetrahedral and octahedral sites.

known difficulty when treating oxide compounds in the DFT-pseudopotential approximation and is also present in  $\alpha$ -alumina.<sup>34</sup> (The theoretical and experimental densities of  $\alpha$ -alumina are also shown in Figure 3 for comparison.) Note that there is a “kink” in the curve near  $n = 0.2$ . This change in slope is a manifestation of the different physical processes at work above and below  $n = 0.2$ . For values of  $n < 0.2$  the H atoms fill nominal spinel cation sites, but for values of  $n > 0.2$  all of the spinel cation sites are full and the H atoms must fill interstitial sites. This latter process has a greater effect on the unit cell, as exhibited by the greater slope in the region  $n > 0.2$ . The experimental density measurements,<sup>21</sup> as well as the X-ray PRF results of Ushakov and Moroz,<sup>23</sup> suggest that the upper limit on the H content in the spinel structure is  $n \approx 0.6$ .

**3.2. Vibrational Frequencies for Interior Hydrogen.** As noted in the Introduction, Tsyganenko et al. have reported bands in the infrared (IR) spectra of  $\gamma$ -alumina<sup>26</sup> at 3300 and 3500  $\text{cm}^{-1}$ . These bands are within the OH-stretching signature region. They assign the experimentally observed IR bands based on the following argument: The band at 3500  $\text{cm}^{-1}$  is more intense and therefore should be assigned to octahedrally coordinated hydrogens, since there are twice as many octahedral sites as tetrahedral ones. We performed calculations of the vibrational frequencies of OH in the  $\text{HAl}_5\text{O}_8$  structure for H in both the nominal tetrahedral and octahedral sites. We expect these frequencies to be characteristic of these two chemical environments throughout the entire sequence of compounds. The computed vibrational frequencies are: H-octahedral = 3306  $\text{cm}^{-1}$  and H-tetrahedral = 3449  $\text{cm}^{-1}$ . The present calculations support an assignment *opposite* to that given by Tsyganenko et al.<sup>26</sup> The calculated total energy is lower by about 0.055 eV, however, when the hydrogens are associated with tetrahedral sites. When this energetic information (unavailable to Tsyganenko et al.) is taken into account, the more intense IR band at 3500  $\text{cm}^{-1}$  should be associated with the lower energy form, which has tetrahedrally coordinated hydrogens, thereby bringing the experimental and theoretical results into excellent agreement. Further confirmation of this reassignment comes from the temperature dependence of the observed IR bands. With increasing temperature the distribution of H will become increasingly statistical as the energy difference between the two forms diminishes relative to the thermal energy. At sufficiently elevated temperatures, adsorption due to octahedrally coordinated H should *exceed* that due to tetrahedrally coordinated H

since there are twice as many octahedral sites. Exactly this reversal in relative absorption intensities upon temperature increase is reported by Tsyganenko et al.<sup>26</sup> The small ( $\sim 1\%$ ) disagreement remaining after the reassignment is well within the error introduced by the harmonic approximation, which was employed in the present calculations.

One further point regarding hydrogen vibrations is worth noting. As discussed above, whether tetrahedrally or octahedrally coordinated, the H ion slides away from the ideal cation site and associates more closely with one of the neighboring O atoms, forming an OH group within the bulk. The above frequencies correspond to H atoms in these preferred OH structures within the bulk. We have also carried out calculations for H atoms placed at the *ideal* tetrahedral and octahedral cation sites. An H atom at an ideal tetrahedral cation site is unstable, but when placed at an ideal octahedral site, the H is in a shallow energy minimum. We computed vibrational frequencies for H in this ideal octahedral site and found that the potential is nearly isotropic, with all three fundamental vibrational frequencies around 220  $\text{cm}^{-1}$ . Experimentally, an IR absorption is observed at about 391  $\text{cm}^{-1}$ , which has been assigned to “hydrogen translation”.<sup>35</sup> Given that the harmonic approximation is generally less reliable for low-frequency vibrations and that there is great difficulty in computing fine energy differences with accuracy, it is difficult to place much importance on the computed result. Nevertheless, it does suggest a possible source for such a low-frequency vibrational mode involving H, and in view of the (rather large) computational uncertainties, the agreement is reasonable.

**3.3. Hydrogen Diffusion through the Bulk.** The density and vibrational frequency calculations corroborate the picture of  $\gamma$ -alumina as a compound for which there is a range of valid H content. Upon thermal treatment,  $\gamma$ -alumina dehydrates and thereby progresses through this range. To further study dehydration, we have investigated the path by which H diffuses through the bulk.

In the spinel structure, the O atoms are cubic close-packed, stacked ABCABC... Tetrahedral and octahedral sites may therefore share a face, as depicted in Figure 4. (In Figure 4, the shared face is defined by O atoms  $\text{O}_2$ ,  $\text{O}_3$ , and  $\text{O}_4$ .)

Our calculations have shown that whether in a nominally tetrahedral or nominally octahedral site, the H atom slides away from the ideal cation site and associates more closely with one of the neighboring O atoms, forming an OH structure. If the H atom is associated with one of the three O atoms at the vertices of the shared face, it may move from the tetrahedral site to the octahedral one simply by “swinging” through the shared face as shown by the arrow marked B in Figure 4. If, however, the H atom is not associated with one of the three O atoms at the vertices of the shared face, it may “hop” to one of those positions as shown by the arrow marked A in Figure 4. To diffuse through the bulk, the H atom follows a “Tarzan mechanism” whereby it takes sequential steps: hop–swing–hop etc. Note that the hop step involves breaking one OH bond and forming another. The swing step does not involve breaking or forming any chemical bonds.

We have computed the energy barrier for each of these two processes and found that the hop step has a higher barrier, about 1.4 eV. To compute this barrier, first single-point total energy calculations were carried out for a grid of geometries mapping out the  $\text{O}_1$ –H distance and the angle  $\text{X}-\text{O}_1$ –H, where X is the ideal tetrahedral site. (X is at the center of the tetrahedron defined by  $\text{O}_1$ ,  $\text{O}_2$ ,  $\text{O}_3$ , and  $\text{O}_4$ .) All grid points were chosen to

(34) Kruse, C.; Finnis, M. W.; Milman, V. Y.; Payne, M. C.; De Vita, A.; Gillan, M. J. *J. Am. Ceram. Soc.* **1994**, *77*, 431.

(35) Saniger, J. M. *Mater. Lett.* **1995**, *22*, 109.

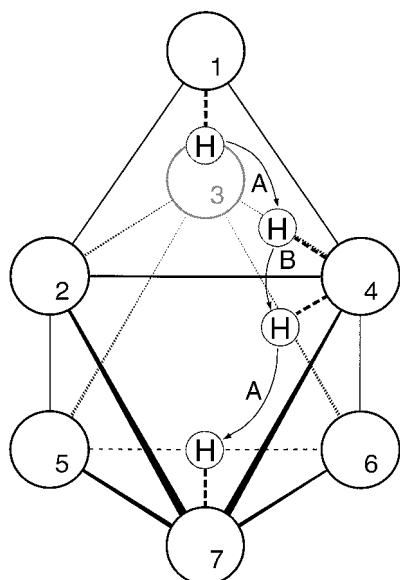


**Figure 4.** Schematic of the key steps to hydrogen diffusion through  $\gamma$ -alumina bulk. Whether in a nominal tetrahedral (upper) or octahedral (lower) site, the H atom associates more closely with one of its neighboring O atoms. If the H atom is associated with an O atom that is shared by adjacent tetrahedral and octahedral sites, it can move from one site to the other by simply “swinging” through the shared face (step B). If the H atom is not associated with one of the shared O atoms, it first must “hop” to one such atom (step A) before it can move from one site to the other. Energetically, step A is more costly.

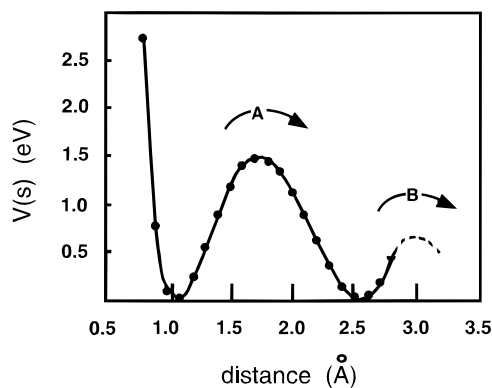


**Figure 5.** Variation in potential along the diffusion “hop” step shown in Figure 4. This step connects two possible H positions within a single tetrahedral site and is the rate-controlling step to H diffusion through bulk  $\gamma$ -alumina. Energy is in eV, distance in Å is the O<sup>1</sup>–H distance along the minimum energy path, shown schematically in Figure 4.

fall in the (O<sub>1</sub>, X, O<sub>4</sub>) plane. Given the computed preferred O–H distance of about 1.0 Å, some simple trigonometry reveals that the two neighboring minima are located at, (R<sub>OH</sub> = 1.0 Å, A<sub>XOH</sub> = 0.0°) and (R<sub>OH</sub> = 2.4 Å, A<sub>XOH</sub> = 22°). The hopping path is easily identified from the resulting potential energy surface and displays the expected minima. The associated one-dimensional potential energy curve along the diffusion path for the hop step is shown in Figure 5. The starting structure employed in these calculations was a fully relaxed one with the H nominally tetrahedrally coordinated. To ascertain the contribution of bulk relaxation during the diffusion, the total energy was recomputed for the structure corresponding to the top of the energy barrier, relaxing all atoms except those defining the size of the unit cell, and the H. The energy decreased by 0.1 eV, suggesting that the effective barrier to H diffusion is lower than the value

given by the rigid scan (shown in Figure 5) by 0.1 eV. The barrier height can then be taken to be about 1.4 eV.

Similar calculations were carried out for the swing step in the diffusion path. The barrier to the swing step was found to be about 0.7 eV. This means that the hop step is much slower than the swing step and therefore limits the rate of H diffusion.

We can estimate the hopping rate as a function of temperature by assuming a Boltzman distribution of energies. Given a barrier height  $\Delta E$ , the fraction of H atoms that have sufficient energy to surmount the hopping barrier at a given temperature  $\rho(E > \Delta E)$  is given by

$$\rho(E > \Delta E) = \frac{1}{kT} \int_{\Delta E}^{\infty} e^{-E/kT} dE \quad (1)$$

Here  $k$  is the Boltzman constant, and  $T$  is the temperature. The hopping rate  $r$  is then simply the rate at which H attacks the barrier, (the vibrational frequency  $\nu$ ) times the probability that it has enough energy to surmount the barrier

$$r = \nu \rho(E > \Delta E) \quad (2)$$

The results of this analysis are entirely consistent with the temperature dependence of the IR spectrum reported by Tsyganenko et al.<sup>26</sup> They found that the OH-stretching bands are unaffected when the temperature is raised from 373 to 400 K, but that appreciable changes in distribution and intensity are present upon heating to 473 K, and H exchange with D is facile at 523 K. Our calculations predict a hopping rate for the H atoms of  $2 \times 10^{-4} \text{ s}^{-1}$  at 400 K (negligible), but  $0.1 \text{ s}^{-1}$  at 473 K, and  $3.4 \text{ s}^{-1}$  at 523 K (appreciable).

#### 4. A Reactive Sponge

The foregoing results lead naturally to the hypothesis that  $\gamma$ -alumina has a most remarkable property which promises to serve as a key to unlock many of the mysteries associated with this material in catalytic processes. Simply put, the material behaves as a sponge, in that it can store and subsequently release water, but in a unique, “reactive” way. When a water molecule arrives at the surface,<sup>36</sup> it breaks up, H enters the bulk, and O stays at the surface. Al atoms countermigrate from the bulk to the surface where they recombine with the new O atoms and extend the crystal matrix. The ratios, determined by valence requirements, work out so that for every three H<sub>2</sub>O molecules, six H move into the bulk, two Al move out, and the crystal extends by a stoichiometric Al<sub>2</sub>O<sub>3</sub> unit. The reverse process is also possible: H comes out from the bulk and combines with surface O to evolve as water, while surface Al countermigrate into the bulk. The net result is an etching of the material as both Al and O atoms leave the surface. Again, the ratios work out the same way so that the etching occurs by stoichiometric Al<sub>2</sub>O<sub>3</sub> units. This unusual chemistry is a natural consequence of the fact that the H content in  $\gamma$ -alumina may fall anywhere within a considerable range ( $0 < n \leq \sim 0.6$ ).

The fact that  $\gamma$ -alumina releases water upon heating has been known for a long time,<sup>21,22,24</sup> but this water has typically been disregarded as simply “residual” from the thermal dehydroxylation of boehmite or from incompletely removed adsorbed water. The latter speculation is motivated in part by the large measured surface area of  $\gamma$ -alumina.<sup>37</sup> It is even conceivable that surface adsorbed water stabilizes  $\gamma$ -alumina with respect

(36) For a detailed account of how H<sub>2</sub>O breaks up on an alumina surface, see ref 50.

(37) McHale, J. M.; Navrotsky, A.; Perrotta, A. J. *J. Phys. Chem. B* **1997**, *101*, 603.

to transformation to  $\alpha$ -alumina, but this supposition has been essentially ruled out by the detailed calorimetric studies of McHale et al.<sup>37</sup> The actual mechanism of water storage only becomes clear when it is recognized that  $\gamma$ -alumina exists over a range of H content, and the rules of valence must be satisfied throughout that range.

Our calculations unequivocally confirm that H is contained within  $\gamma$ -alumina bulk: The density profile is correct, the IR bands are properly predicted, and the temperature dependence of hydrogen mobility agrees with experimental observations. Since the final dehydration product does *not* contain H, the H in the evolving water must come from the bulk, but since *water* is driven off, O has to come from somewhere! There are only three possible sources of O. The O can come from the bulk, from the surface, or from the environment outside the surface; however, as we will now discuss, only one of these sources, the surface, does not conflict with known data.

The first possibility is that the O also comes from the bulk. This would mean that O actually diffuses out from within the alumina along with H. X-ray data show, however, that throughout the dehydration process the spinel structure is maintained.<sup>24</sup> Since the "water from within the bulk" mechanism would destroy the CCP oxygen structure, it is inconsistent with the X-ray data.

The second possibility is that when the diffusing H atoms reach the surface they pick up O from the environment, (from O<sub>2</sub> or O-containing species in the air for example). This would leave the CCP O structure unchanged, but the stoichiometry of the resulting dehydrated species would be wrong.  $\text{HAl}_5\text{O}_8$  would dehydrate to  $\text{Al}_5\text{O}_8$ .

In the postulated "surface etching" mechanism the stoichiometry is properly maintained. Furthermore, to maintain the balance of valence, Al atoms must migrate into one-third of the holes left by the departing H atoms. The "surface etching" mechanism described above provides a driving force for this countermigration of Al. As H picks up O at the surface and leaves as H<sub>2</sub>O, it leaves behind a surface rich in Al compared to the bulk. The concentration gradient will then drive some Al into the bulk. No other possible source of O would facilitate this (essential) countermigration of Al. Finally, if O is taken from the surface, the CCP O structure of the bulk is left unchanged, in agreement with experiments.

There are several possible significant implications of the unusual surface chemistry described above. First, the availability of atomic H and O at the surface is likely to facilitate *both* oxidation and reduction, providing a clue to its success in automotive three-way catalysts (TWC),<sup>10</sup> which must perform simultaneous oxidation and reduction. Second, since catalysts are often formed by dispersal of transition-metal atoms on an insulating support surface,  $\gamma$ -alumina being the carrier of choice, it is thought that diffusion of the metal atoms into the support represents a potential degradation mechanism.<sup>38</sup> Certainly support-metal interactions are known to play a critical role in determining the efficacy of catalytic activity.<sup>9,39,40</sup> In view of the "surface etching" mechanism for dehydration, it is probable that entrapment of ultradispersed metal atoms in the surface vacancies created in the etching process may leave them unavailable to assist catalysis.

## 5. Structure of Spinel Aluminas

**5.1.  $\gamma$ - and  $\eta$ -Alumina.** It is enlightening to consider the range of possible distributions for the cation vacancies in the

**Table 1.** Reported Distributions of Al over Tetrahedral and Octahedral Sites in the Assumed Defect Spinel Structure of  $\gamma$ -Alumina<sup>a</sup>

method	date	$x_{Td}$	ref	comment
X-ray	1935	37.5	47	all vacancies $O_h$
X-ray	1958	37.5	47	vacancies probably $O_h$
thought expt.	1960	~25	47	$T_d$ sites hardly occupied
electron diffraction	1965	25	47	
X-ray	1969	25 ↔ 37.5	1	temperature dependent
<sup>27</sup> Al NMR	1983	25	41	
X-ray	1991	25	24	all vacancies $T_d$
pair-potential	1997	37.5	49	vacancies prefer $O_h$ by 3.7 eV
<sup>27</sup> Al NMR	1997	30.1	42	

<sup>a</sup> The reported value ( $x_{Td}$ ) is the % of Al atoms that are tetrahedrally coordinated. Within the restrictions imposed by the spinel lattice and the  $\text{Al}_2\text{O}_3$  stoichiometry, the fraction of Al that is octahedrally coordinated ( $x_{Oh}$ ) can not fall outside the range [ $62.5\% \leq x_{Oh} \leq 75\%$ ].

fully dehydrated structure. As noted in the Introduction, the stoichiometry demands one cation vacancy out of nine cation sites. To consider the range of possible distributions for the cation vacancies, we start from the Mg spinel primitive cell ( $\text{Mg}_2\text{Al}_4\text{O}_8$ ), and multiply by 1.5 to gain a formula with exactly nine cations, ( $\text{Mg}_3, \text{Al}_6\text{O}_{12}$ ). (Here the comma separates the  $T_d$  and  $O_h$  species.) Replacing the Mg with Al and introducing one cation vacancy, we can produce two limiting structures: ( $\square\text{Al}_2, \text{Al}_6\text{O}_{12}$ ) in which case all of the vacancies occupy tetrahedral ( $T_d$ ) sites and 75% of the cations are octahedrally ( $O_h$ ) coordinated, or ( $\text{Al}_3, \square\text{Al}_5\text{O}_{12}$ ) in which case all of the vacancies occupy octahedral sites and only 62.5% of the cations are octahedrally coordinated. It is important to note that these represent limiting cases. Within the restrictions imposed by the spinel lattice and the  $\text{Al}_2\text{O}_3$  stoichiometry, the fraction of the Al that is octahedrally coordinated ( $x_{Oh}$ ) cannot fall outside the range [ $62.5\% \leq x_{Oh} \leq 75\%$ ]. Table 1 collects various results which have been reported concerning the distribution of vacancies. Note in particular that despite decades of research, no consensus has emerged regarding the distribution of vacancies. It is perhaps also an important observation that all but two of the reports found  $x_{Oh}$  to lie at one extreme or the other of the physically allowed range.

<sup>27</sup>Al NMR studies<sup>41</sup> found  $75 \pm 4\%$  Al coordinated  $O_h$  in  $\gamma$ -alumina and  $65 \pm 4\%$  Al coordinated  $O_h$  in  $\eta$ -alumina. More recent work corroborates this result.<sup>42</sup> Detailed X-ray studies also support a preference for vacancies at tetrahedral sites in  $\gamma$ -alumina and at octahedral sites in  $\eta$ -alumina.<sup>24</sup> Given the above-mentioned limiting cases, it is clear that  $\gamma$ -alumina is the structure with H at tetrahedral sites, dehydrating to ( $\square\text{Al}_2, \text{Al}_6\text{O}_{12}$ ), and  $\eta$ -alumina is the structure with H at octahedral sites that dehydrates to ( $\text{Al}_3, \square\text{Al}_5\text{O}_{12}$ ). We have computed fully relaxed (energetically minimized) structures for  $\eta_{0.2}$ -alumina and  $\gamma_{0.2}$ -alumina. We find  $\eta$ -alumina to be the higher energy species. This is consistent with the fact that greater disorder is observed in  $\eta$ -alumina.<sup>3</sup> This picture is also consistent with the nature of the precursor materials.  $\gamma$ -Alumina comes from dehydration of boehmite.<sup>43</sup>  $\eta$ -Alumina comes from dehydration of bayerite.<sup>16</sup> John<sup>41</sup> reported that boehmite has a higher fraction of octahedrally coordinated Al than does bayerite.

It must be acknowledged that the above limiting cases represent *ideal* forms. Any real sample will certainly have

(40) Hoost, T. E.; Otto, K.; Laframboise, K. A. *J. Catal.* **1995**, *155*, 303.

(41) John, C. S.; Alma, N. C. M.; Hays, G. R. *Applied Catal.* **1983**, *6*, 341.

(42) Lee, M.-H.; Cheng, C.-F.; Heine, V.; Klinowski, J. *Chem. Phys. Lett.* **1997**, *265*, 673.

(38) Yao, H. C.; Japar, S.; Shelef, M. *J. Catal.* **1977**, *50*, 407.

(39) Oh, S. H.; Eickel, C. C. *J. Catal.* **1991**, *128*, 526.



disorder, defects, etc. For example, evidence suggests that in  $\eta$ -alumina, a small fraction of the Al atoms occupy the 16(c) and 48(f) sites of  $Fd3m$ .<sup>44</sup> In fact, the effects of disorder in real samples must be of the same order as the effects of the subtle difference in the distribution of vacancies because  $\gamma$ -alumina and  $\eta$ -alumina have often been regarded as identical.<sup>45,46</sup>

**5.2.  $\gamma$ - and  $\delta$ -Alumina.** Some may argue that the H-free form is the only "true"  $\gamma$ -alumina, but it is probable that  $n = 0.0$  corresponds to a different transition form. It has been suggested<sup>21</sup> that the transition to another form such as  $\theta$ -alumina or  $\delta$ -alumina may take place prior to complete thermal dehydration of  $\gamma$ -alumina. In fact,  $\delta$ -alumina follows  $\gamma$ -alumina in the boehmite  $\rightarrow$  corundum sequence.<sup>16</sup> The structure of  $\delta$ -alumina is known to be based on a triple block of spinels.<sup>16,47,48</sup> A triple block of spinels, however, gives rise to precisely the structure that is usually called defect spinel. For example, the limit  $n = 0$  in  $\text{Al}_2\text{O}_3 \cdot n\text{H}_2\text{O}$  corresponds to three units of  $\text{HAl}_5\text{O}_8$ , with the three H replaced by an Al and two vacancies. The formula which results,  $\square\text{Al}_{16}\text{O}_{24}$ , is one for which the equivalence to the empirical formula  $\text{Al}_2\text{O}_3$  is transparent. It is typically written with the cumbersome  $\square_{2^{2/3}}\text{Al}_{21^{1/3}}\text{O}_{32}$ . (Note that  $2^{2/3}:21^{1/3}:32 = 2:16:24$ ). The formula with fractional subscripts has been used universally and refers to atoms in a cubic cell. Our much simpler description refers to atoms in *three primitive cells* of Mg spinel. The above analysis makes it clear that  $\gamma$ -alumina is a H-containing form, because complete dehydration while maintaining the spinel structure produces the triple block superstructure assigned to  $\delta$ -alumina. Calculations for the triple block  $\delta$  structure are included in Figure 2.

Our new formula has important consequences for atomic-scale calculations. We note that the most recent electronic structure calculation reported for the defect spinel structure<sup>49</sup> adopted a cubic cell with 32 O atoms, 21 Al atoms, and 3 cation vacancies as a tolerable approximation to the stoichiometric  $\square_{2^{2/3}}\text{Al}_{21^{1/3}}\text{O}_{32}$ . More accurate and faster calculations could have been done with a cell containing 24 O atoms, 16 Al atoms, and two cation vacancies.

## 6 Conclusions

DFT quantum mechanical calculations have been applied to study the dehydration of  $\gamma$ -alumina. Three sets of calculations were carried out. First, fully relaxed structures (including unit

cell optimization) were computed for  $\gamma$ -alumina at various levels of dehydration. These calculations provide an energy profile for dehydration of  $\gamma$ -alumina and demonstrate that  $\text{HAl}_5\text{O}_8$  is a special form. In addition, these calculations provide a theoretical estimate of the material density as a function of the degree of dehydration, and the results are in good accord with experiment. Second, vibrational frequencies were computed for H atoms within the bulk. Vibrational frequencies were computed for H atoms in nominal tetrahedral and nominal octahedral sites. When compared with IR spectra from the literature, excellent agreement is found, although a reinterpretation of the experimental spectra based on new energetic data is first required. Third, the energy barrier to diffusion of H through the bulk was computed. It is found that the rate-limiting step for diffusion of H through the bulk is a "hop" along the O—O edge of a nominal spinel cation site. The barrier to this hop is found to be 1.4 eV, and this predicts a temperature dependence for H mobility in excellent agreement with experimental results.

The picture that results from our calculations is one in which  $\gamma$ -alumina exists with *varying amounts of hydrogen within the bulk*. The terminus of this sequence is the widely accepted defect spinel structure for  $\gamma$ -alumina, a structure which is based on a triple block of spinel primitive cells and is more correctly associated with  $\delta$ -alumina. We have shown that understanding the distribution of cation vacancies unveils the relationship among several transition aluminas. This relationship is supported by <sup>27</sup>Al NMR data from the literature.

Finally, the formula  $\text{H}_{3m}\text{Al}_{2-m}\text{O}_3$  captures a fascinating property of  $\gamma$ -alumina; it behaves rather like a sponge, but with the peculiar property that water is decomposed or reconstituted at the surface. All of this chemistry is a natural consequence of maintaining proper valence over a range of stoichiometries with different H content while simultaneously maintaining the spinel structure. The availability of atomic H and O at the surface is likely to have significant implications in understanding the remarkable catalytic properties of  $\gamma$ -alumina.<sup>2,26</sup>

**Acknowledgment.** We thank K. Hass of the Ford Research Laboratory for useful discussions and Lou Hector of Alcoa Inc. for a copy of ref 16. This work was supported by the U.S. Department of Energy, Office of Basic Energy Sciences under contract No. DE-AC05-96OR22464 with the Lockheed-Martin Energy Research Corporation, by the National Science Foundation Grant DMR-9803768, and by the William A. and Nancy F. McMinn Endowment at Vanderbilt University. Computations were partially supported by the National Center for Supercomputing Applications (NCSA) under Grant DMR980007N to K.S. and utilized the SGI Power ChallengeArray at NCSA, University of Illinois at Urbana-Champaign, K.S. was supported by an appointment to the ORNL Postdoctoral Research Program administered jointly by ORNL and Oak Ridge Associated Universities.

JA991098O

(43) Wilson, S. J. *J. Solid State Chem.* **1979**, *30*, 247.

(44) Ernst, F.; Pirouz, P.; Heuer, A. H. *Philos. Mag. A* **1991**, *63*, 259.

(45) Drago, A. L.; Diamond, J. J. *J. Am. Ceram. Soc.* **1967**, *50*, 568.

(46) Thorton, J. A.; Chin, J. *Am. Ceram. Soc. Bull.* **1977**, *56*, 504.

(47) Lippens, B. C.; Steggerda, J. J. In *Physical and Chemical Aspects of Adsorbents and Catalysts*; Linsen, B. G., Ed.; Academic Press: London, 1970.

(48) Narayanan, C. R.; Srinivasan, S.; Datye, A. K.; Gorte, R.; Biaglow, A. *J. Catal.* **1992**, *138*, 659.

(49) Mo, S-D.; Xu, Y.-N.; Ching, W.-Y. *J. Am. Ceram. Soc.* **1997**, *80*, 1193.

(50) Hass, K. C.; Schneider, W. F.; Curioni, A.; Andreoni, W. *Science* **1998**, *282*, 265.